Full-Speed Sensorless Control Scheme for Permanent Magnet Synchronous Motor Using Artificial Neural Network

Hasan Ali Gamal Al-kaf[1], Sadeq Ali Qasem Mohammed[1] and Kyo-Beum Lee[1]

[1] Department of Electrical and Computer Engineering, Ajou University, Suwon, South Korea

Abstract-- **Extended back electromotive force (EEMF) has been widely used as speed estimation of permanent magnet synchronous motors (PMSMs) due to its excellent performance at medium and high speeds. However, at low speed, EEMF method has low estimation accuracy. Several sensorless methods have combined EEMF with different accurate low-speed estimation techniques to attain a satisfactory estimation performance in the whole speed range. However, the transition between EEMF and low-speed estimation methods is a crucial step that requires two separate speed estimators with different structures. This leads to increased design complexity. Therefore, in this paper, a single sensorless full-speed control is proposed using an artificial neural network (ANN). The proposed ANN method does not require any transition method compared with hybrid full-speed sensorless methods. Simulation results show that proposed ANN can estimate rotor position for full speed compared with EEMF which estimates the rotor speed at medium and high speed.**

***Index Terms*— artificial neural network, Extended back electromotive force, Sensorless methods, PMSM.**

I. INTRODUCTION

Permanent magnet synchronous motors (PMSMs) have replaced induction motors (IM) due to their several advantages, e.g., high efficiency and prevents losses during flux generation, high torque, compact size, and better power density, etc. [1]. In addition, they have been widely employed in various industrial applications which can be effectively regulated via a number of control approaches including model predictive control (MPC) and field-oriented control (FOC) [2]. However, these approaches require the rotor position and speed using the installation of a mechanical encoder or resolver mounted on the shaft of the rotor. The main disadvantages of the installation of such sensors are increasing the volume and the cost, space, and continuous maintenance of motor drives [3–5]. Therefore, several position sensorless methods have been implemented over the past three decades.

The most common estimation method for industrial applications is based on the extended back electromotive force (EEMF) which require a simple and fewer calculation method. EEMF offers accurate position and speed estimation when the motor operates in the high-speed region. However, at zero and low speed, the EEMF method has low estimation accuracy due to the EEMF of the motor reduces proportionally to the speed of the rotor.

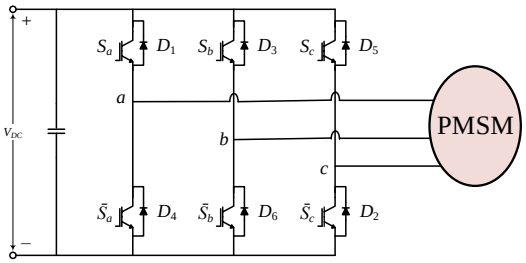

Fig. 1. Two-level voltage source inverter circuit.

Several senseless methods have been introduced to overcome this limitation [6-16]. The main natural solution is to combine EEMF with different accurate estimation techniques for low-speed in order to attain an estimator performing well in the whole speed range. In [6], [7], and [8] have proposed hybrid techniques for sensorless control in electric motors. In [6], the authors present a method that uses low-speed estimates provided by indirect flux detection by online reactance measurement (INFORM) and combines it with an EMF-based observer. EEMF techniques integrated with high frequency signal injection was proposed in [7]. In [8] describes a technique that combines a current injection method and an EMF estimator. However, the ability to control the transition from low speed to high speed without using sensors is a crucial step in achieving accurate full-speed estimation. Moreover, traditional full-speed sensorless techniques require two separate position estimators with different structures to be used at different speeds. This leads to increased design and tuning efforts and makes the control algorithm more complex [17]. The hybrid speed sensorless control methods lack versatility across different speed ranges. A more desirable solution for the industry would be to have a single sensorless control algorithm that can be used for full-speed control.

Conversely, the use of data-driven methodologies, particularly artificial neural network-based (ANN) approaches, is rapidly expanding in the field of power electronics and drives [18–20]. In this study, a single sensorless control algorithm for full-speed control is proposed using ANN. The proposed ANN does not require

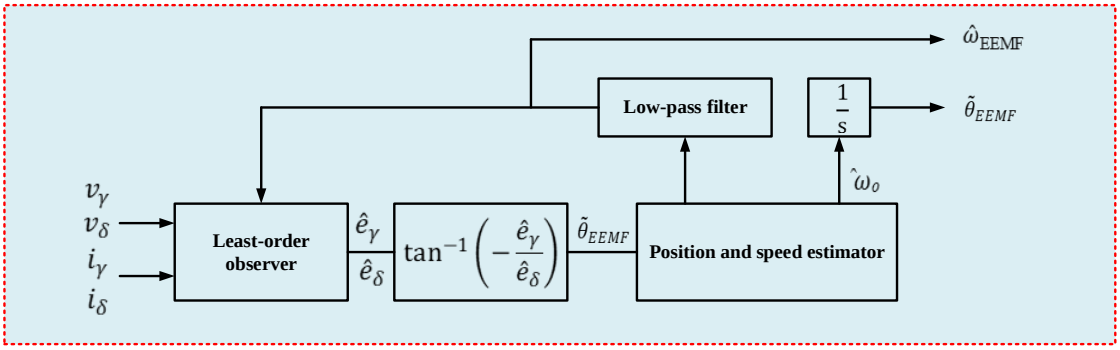

Fig. 2. The block diagram of the EEMF method.

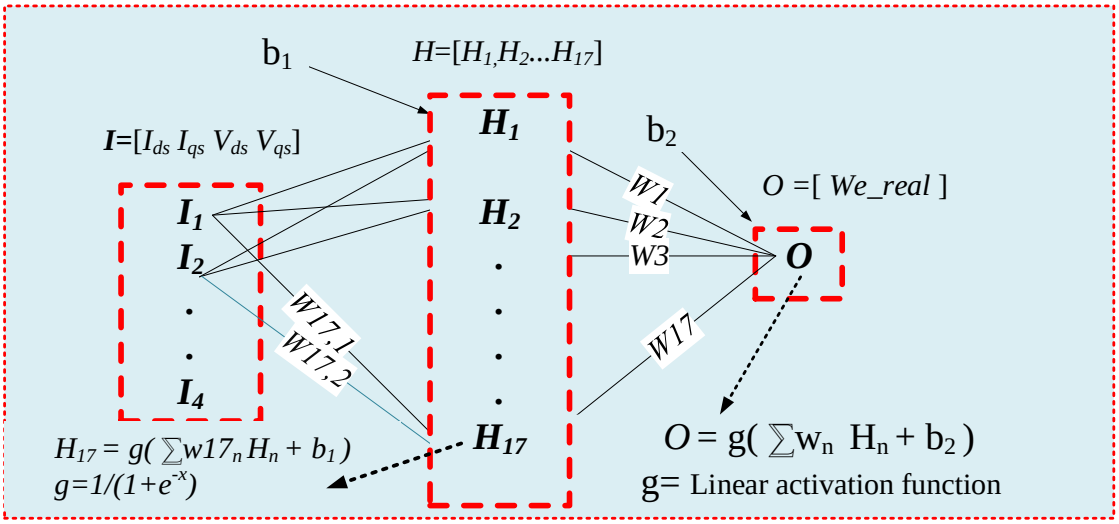

Fig. 3. The block diagram of the proposed MLNN.

a transition between controls which provides a low complex system. Simulation findings shows that the proposed model ANN has a better estimation than EEMF in low-speed regions. In addition, the proposed ANN can estimate rotor position for full speed compared with EEMF which estimates the rotor speed at medium and high speed only.

II. Extended Back Electromotive Force

The method based on an EEMF calculates the rotor position and speed considering the direct proportionality between the EMF and the rotor speed. Surface-mounted PMSM is used in this study using a two-level inverter as shown in Fig 1. Assume that difference between L_d and L_q is small, equation (1) can be expressed as follow

$$\begin{bmatrix} v_d \\ v_q \end{bmatrix} = \begin{bmatrix} R_s + pL_q & -\omega_r L_d \\ \omega_r L_d & R_s + pL_q \end{bmatrix} \begin{bmatrix} i_d \\ i_q \end{bmatrix} + \begin{bmatrix} 0 \\ e_{EEMF} \end{bmatrix}, \quad (1)$$

where e_{EEMF} is an extended EMF. When converting equation (1) from the rotating d-q reference frame to the estimated stationary frame, the estimated voltage equation are represented as:

$$\begin{bmatrix} v_\gamma \\ v_\delta \end{bmatrix} = \begin{bmatrix} R_s + pL_d & -\omega_r L_q \\ \omega_r L_q & R_s + pL_d \end{bmatrix} \begin{bmatrix} i_\gamma \\ i_\delta \end{bmatrix} + \begin{bmatrix} e_\gamma \\ e_\delta \end{bmatrix}, \quad (2)$$

$$\begin{bmatrix} e_\gamma \\ e_\delta \end{bmatrix} = e_{EEMF} \begin{bmatrix} -\sin\tilde{\theta}_{EEMF} \\ \cos\tilde{\theta}_{EEMF} \end{bmatrix} \begin{bmatrix} i_\gamma \\ i_\delta \end{bmatrix} + \left(\hat{\omega}_{\text{EEMF}} - \omega_r\right) \begin{bmatrix} -i_\delta \\ i_\gamma \end{bmatrix} \quad (3)$$

e_γ and e_δ denote the EEMFs measured on stationary reference frame. The estimated speed using the EEMF method is represented by $\hat{\omega}_{\text{EEMF}}$, while the actual speed of the rotor is denoted by ω_r . The extended e_γ and $e_\delta$denote, are estimated through a least order observer. If the error between the estimated speed $\hat{\omega}_{\text{EEMF}}$, and the actual speed ω_r, is minimal, the relationship between the estimated extended EMF and the position error of the stationary reference frame $\tilde{\theta}_{EEMF}$, can be characterized as follows.

$$\begin{bmatrix} \hat{e}_\gamma \\ \hat{e}_\delta \end{bmatrix} = e_{EEMF} \begin{bmatrix} -\sin\tilde{\theta}_{EEMF} \\ \cos\tilde{\theta}_{EEMF} \end{bmatrix}, \tilde{\theta}_{EEMF} = \tan^{-1}\left(-\frac{\hat{e}_\gamma}{\hat{e}_\delta}\right). \quad (4)$$

The calculated value of $\tilde{\theta}_{EEMF}$ from equation (4) is utilized to estimate the rotor position using a position-speed estimator. A proportional-Integral (PI) controller is employed to calculate the estimated speed, $\hat{\omega}_o$. By

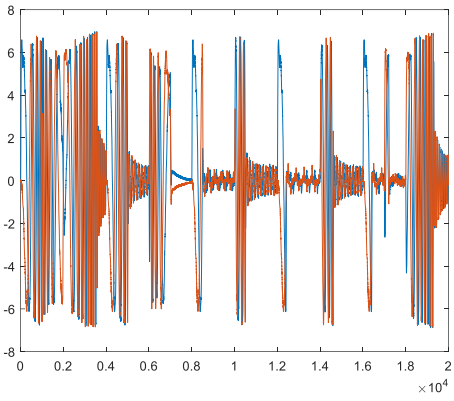

(a)

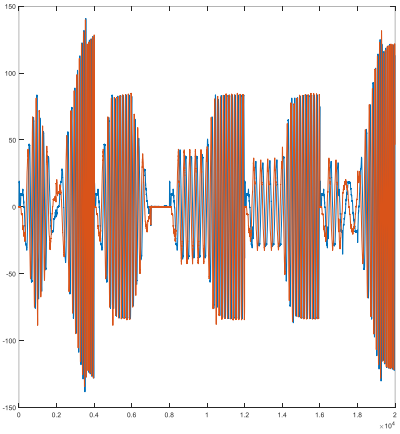

(b)

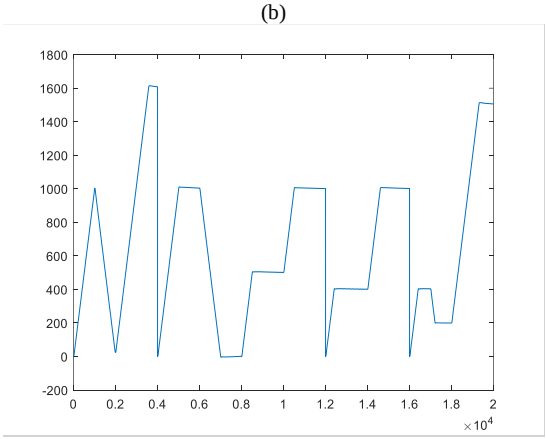

(c)

Fig. 4. Input-target data collection: (a) I_{dqs} (b)V_{qds} (c) speed.

integrating this estimated value, the position of $\tilde{\theta}_{EEMF}$ is determined. The actual control of the PMSM is performed using the estimated speed, $\hat{\omega}_{\text{EEMF}}$, which is obtained by applying a low-pass filter to $\hat{\omega}_o$. A block diagram of the position and speed estimation algorithm based on the extended EMF is shown in Fig. 2.

III. Proposed Sensorless Speed Estimation

A multilayer neural network (MLNN) with Levenberg Marquardt is used to estimate the full speed for PMSM.

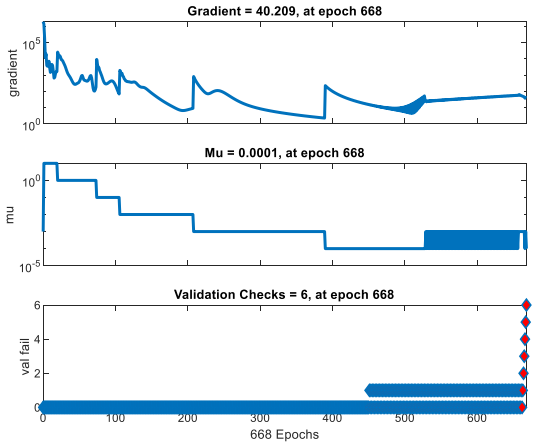

Fig. 5. Matlab simulation result of optimal epoch.

Fig. 3 shows the block diagram of the proposed MLNN. In the first step, we collected data from speed control for PMSM. The input parameters are I_{ds}, I_{qs}, $V_{ds,}$ and V_{qs} in a stationary reference frame, where the target is the actual speed (ω_r). The data is taken for different ranges of speed in order to cover all the operational conditions. The data is collected under low, medium and high speed with different v_{dqs} voltages and I_{dqs} current in stationary reference frame s as illustrated in Fig 4.

Then, using MATLAB software, the collected data is split into training, validation and testing, and MLNN parameters are initialized such as the activation function is the sigmoid function and linear function for hidden and output layer, respectively, the hidden neuron is set to 17 and only one hidden layer is used as shown in Table I. The training of proposed MLNN is done offline to avoid the large computation time for the training process. The

TABLE I. ANN Parameters

MLNN method	**Value**
Number of input	4
Number of layer in hidden layer	1
Number of neuron in hidden layer	17
Number of output	1
Active function of hidden layer	Sigmoid
Active function of output layer	Purelin
Training algorithm	Trainlm
Number of iterations	1000
Training percentage	70%
Validation percentage	15%
Testing percentage	15%
Normalization method	Minmax
Metrix evaluation	Mean square error

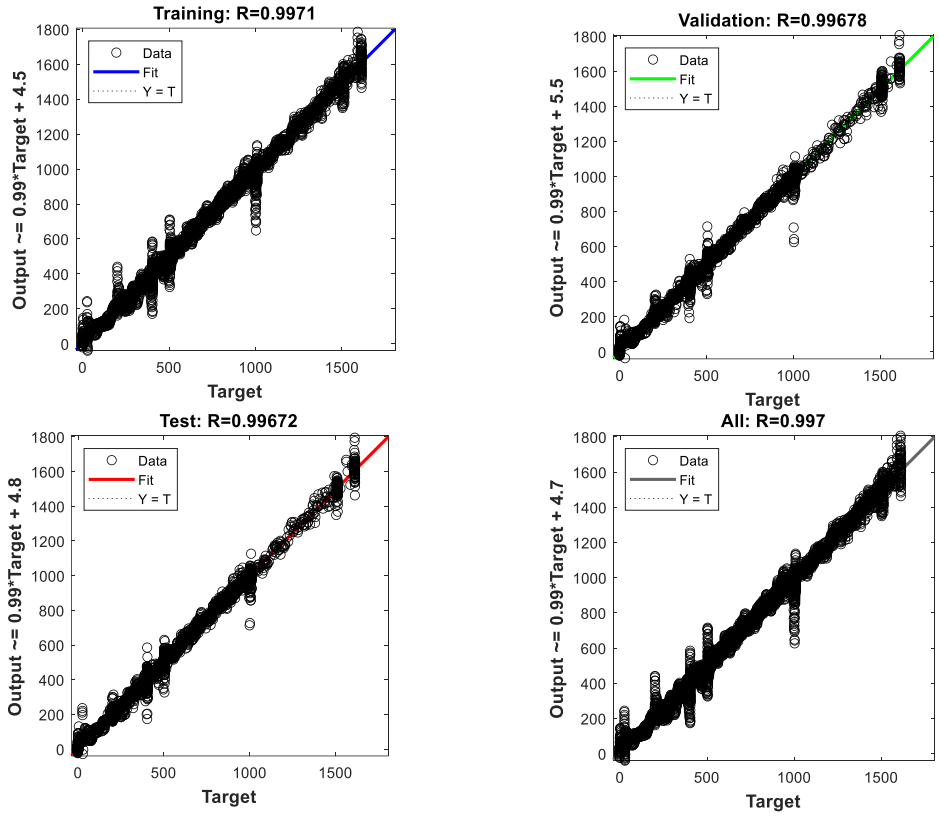

Fig. 6. Matlab simulation results of correlation coefficient for training, validation, testing and overall performance.

Levenberg Marquardt is used due to its fast convergence, high accuracy, and required low number of iterations. Fig. 5 shows the iteration that has the best performance was 668 with gradient and mutation value.

The proposed methods show high performance with a correlation coefficient of above 0.99 for all training, validation, and testing sets as shown in Fig 6. In detail, the correlation coefficient for training, validation, and testing were 0.9971, 0.9970, and 0.9967, respectively. The overall correlation coefficient was 0.9970.

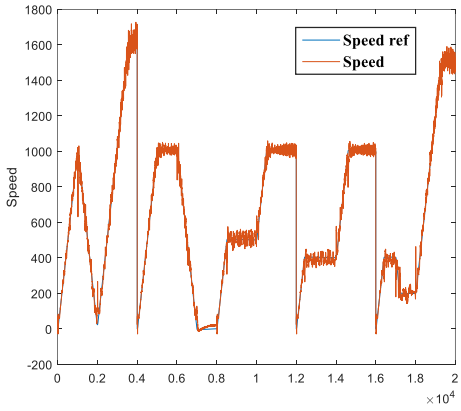

Fig. 7. Matlab simulation result for speed estimation using MLNN.

Once the MLNN can predict the actual speed accurately, a simple mathematical equation of MLNN is used in real-time without the computation complexity of the training algorithm which provides a fast estimation response. The optimal weight and bias are extracted and it multiplies with inputs and activation functions. The outcome of the multiplication is the speed. The position of $\tilde{\theta}_{ANN}$ is obtained by integrating speed estimation.

IV. Simulation Results

The simulation results were done using PSIM and Matlab software. Table II lists the parameters of the PMSM used in this simulation. Fig 7. shows the speed ref and speed estimation using MLNN under different speed regions including low, medium and high speed. The result shows that the speed estimation by MLNN follow exactly the speed ref at sharp variation of speed value which prove the robustness of the proposed method. However, there is slight different between the speed ref and speed estimation at some value which could be solve using including large training dataset. Once the MLNN can predict the actual speed accurately using Matlab software, a simple mathematical equation of MLNN is used in PSIM without the computation complexity of the training algorithm which provides a fast estimation response. Fig 8a compares the estimated position and speed obtained through the use of an EEMF technique and an MLNN

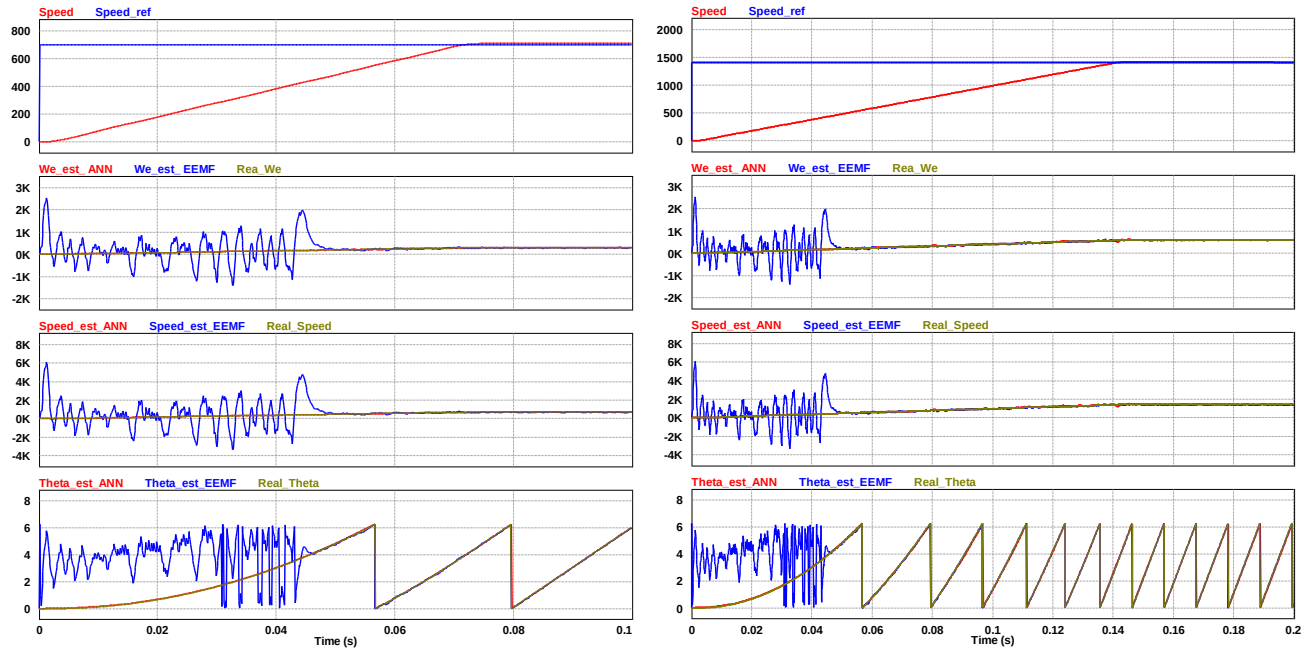

(a) (b)

Fig. 8. PSIM simulation result for position and speed estimation using EEMF and MLNN: (a) low-medium regions (b) low to high speed regions

approach during low to medium and low to high speed, respectively. PMSM is controlled using information from a sensor to determine the rotor's position. The speed of the PMSM was gradually increased starting from 0 rpm. From Fig 8a, it can be seen that the EEMF has poor speed and position estimation during low-speed operation. On the other hand, MLNN method demonstrates superior accuracy in estimating both position and speed due to the ability of ANN methods to effectively capture nonlinear characteristics. Simulation results of rotor position estimation at low to high speeds are presented in Figs 8b. The results reveal the estimation accuracy of the EEMF-based method during medium-speed operation when the speed is raised from 500 rpm. The EEMF method maintains stable performance when the rotor speed and EMF are high. Additionally, the MLNN method is capable of estimating the rotor position at medium and high speeds, however, the EEMF method shows a better performance compared to the MLNN. According to Fig 9, there are two full-speed regions: 0 to 700 and 700 to 1400 rpm. The result indicates that the EEMF Method struggles to estimate speed and position accurately in the range of 0 to 350 rpm. This difficulty arises from the proportional reduction in the ability to estimate the EEMF of the motor with decreasing rotor speed. On the other hand, the MLNN exhibits superior performance at low speeds. This advantage is attributed to the MLNN's learning process, which involves training MLNN using actual speed, current, and voltage values in a stationary state. Consequently, the MLNN does not rely heavily on the proportionate effect of the EEMF value. Conversely, the EEMF method demonstrates better performance than MLNN during medium and high speeds. However, there is room for further improvement in this range, which could be achieved by implementing a larger training dataset or applying advanced machine learning techniques.

TABLE II
SIMULATION PARAMETERS

Parameters	Value
DC-link voltage (V_{dc})	600V
Rated Power	5kw
Pole (P)	8
Inertia (J)	0.00666Kg·m^2
d-axis inductance (L_d)	0.00729H
q-axis inductance (L_q)	0.00725H
Stator resistance (R_s)	0.158Ω
Magnetic flux linkage (φ_f)	0.264Wb
Rated speed	1750rpm
Sampling time (T_{samp})	100μs

V. CONCLUSIONS

A single sensorless control method for full-speed control is proposed using ANN. The proposed ANN method does not require any transition method compared with the hybrid method. Simulation results show that the proposed ANN can estimate rotor position for full speed compared with EEMF which estimates the rotor speed at medium and high speed only.

ACKNOWLEDGMENT

This work was supported by the Korea Institute of Energy Technology Evaluation and Planning (KETEP) and the Ministry of Trade, Industry & Energy (MOTIE) of the Republic of Korea (No. 20206910100160).

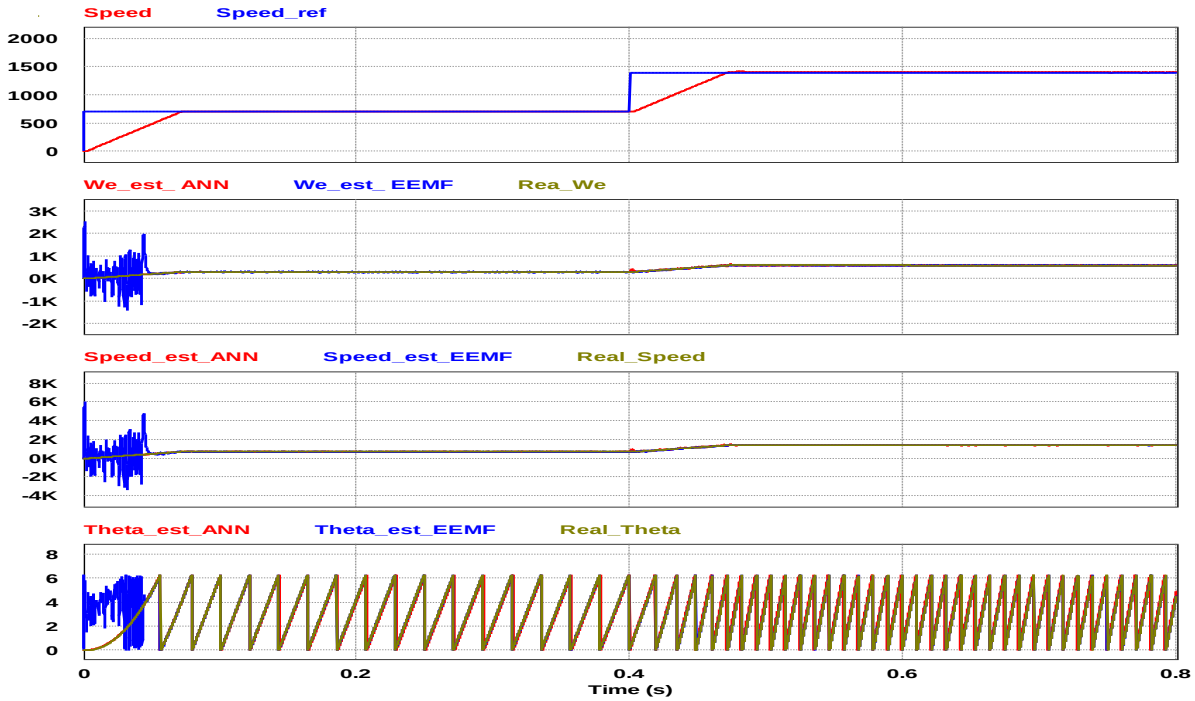

Fig. 9. PSIM simulation result for position and speed estimation using EEMF and MLNN for full speed regions.

REFERENCES

[1] Y. Yao, Y. Huang, F. Peng, J. Dong, and H. Zhang, "An improved deadbeat predictive current control with online parameter identification for surface-mounted PMSMs," *IEEE Trans. Ind. Electron.*, vol. 67, no. 12, pp. 10145–10155, Dec. 2020.

[2] H. A. G. Al-kaf, S. S. Hakami and K. -B. Lee, "Hybrid current controller for permanent-magnet synchronous motors using robust switching techniques," *IEEE Trans. Power Electron.*, vol. 38, no. 3, pp. 3711-3724, Mar. 2023.

[3] D. Liang, J. Li, and R. Qu, "Sensorless control of permanent magnet synchronous machine based on second-order sliding-mode observer with online resistance estimation," *IEEE Trans. Ind. Appl.*, vol. 53, no. 4, pp. 3672–3682, Jul./Aug. 2017.

[4] Z. Xu, T. Zhang, Y. Bao, H. Zhang, and C. Gerada, "A nonlinear extended state observer for rotor position and speed estimation for sensorless IPMSM drives*," IEEE Trans. Power Electron*., vol. 35, no. 1, pp. 733–743, Jan. 2020.

[5] Y. Lee and S. K. Sul, "Model-based sensorless control of an IPMSM with enhanced robustness against load disturbances based on position and speed estimator using a speed error," *IEEE Trans. on Ind. Appl*., vol. 54, no. 2, pp. 1448–1459, Mar./Apr. 2018.

[6] U. Rieder, M. Schroedl, and A. Ebner, "Sensorless control of an external rotor PMSM in the whole speed range including standstill using DC-link measurements only," *in Proc. IEEE 35th Annu. Power Electron. Spec. Conf.*, 2004, vol. 2, pp. 1280–1285.

[7] J. Lara, A. Chandra, and J. Xu, "Integration of HFSI and extended-EMF based techniques for PMSM sensorless control in HEV/EV applications," *in Proc. 38th Annu. Conf. IEEE Ind. Electron. Soc*., 2012, pp. 3688–3693.

[8] M. Seilmeier and B. Piepenbreier, "Sensorless control of PMSM for the whole speed range using two-degree-of-freedom current control and HF test current injection for low-speed range," *IEEE Trans. Power Electron.*, vol. 30, no. 8, pp. 4394–4403, Aug. 2015.

[9] D. Xiao et al., "Universal full-speed sensorless control scheme for interior permanent magnet synchronous motors," *IEEE Trans. Power Electron*., vol. 36, no. 4, pp. 4723–4737, Apr. 2021.

[10] S. C. Yang and Y. L. Hsu, "Full speed region sensorless drive of permanent-magnet machine combining saliency-based and back-EMFbased drive," *IEEE Trans. Ind. Electron*., vol. 64, no. 2, pp. 1092–1101, Feb. 2017.

[11]] J. Lara, A. Chandra, and J. Xu, "Integration of HFSI and extended-EMF based techniques for PMSM sensorless control in HEV/EV applications," *in Proc. 38th Annu. Conf. IEEE Ind. Electron*. Soc., 2012, pp. 3688–3693.

[12] Z. Zhao, C. Hu, Z. Wang, S. Wu, Z. Liu, and Y. Zhu, "Back EMF-based dynamic position estimation in the whole speed range for precision sensorless control of PMLSM," *IEEE Trans. Ind. Inform*., vol. 19, no. 5, pp. 6525–6536, May. 2023.

[13] S. Morimoto, K. Kawamoto, M. Sanada, and Y. Takeda, "Sensorless control strategy for salient-pole PMSM based on extended EMF in rotating reference frame," *IEEE Trans. Ind. Appl*., vol. 38, no. 4, pp. 1054–1061, Jul./Aug. 2002.

[14] F. Genduso, R. Miceli, C. Rando, and G. Galluzzo, "Back EMF sensorless-control algorithm for high dynamic performance PMSM," *IEEE Trans. Ind. Electron*., vol. 57, no. 6, pp. 2092–2100, Jun. 2010.

[15] E. Robeischl, M. Schroedl, and M. Krammer, "Position-sensorless biaxial position control with industrial PM motor drives based INFORM and back EMF model," *in Proc. IEEE IECON'02*, 2002, pp. 668–673.

[16] X. Song, J. Fang, B. Han, and S. Zheng, "Adaptive compensation method for high-speed surface PMSM sensorless drives of EMF-based position estimation error," *IEEE Trans. Power Electron*., vol. 31, no. 2, pp. 1438–1449, Feb. 2016.

[17] D. Xiao et al., "Universal full-speed sensorless control scheme for interior permanent magnet synchronous motors," *IEEE Trans. Power Electron*., vol. 36, no. 4, pp. 4723–4737, Apr. 2021.

[18] H. A. G. Al-Kaf and K. -B. Lee, "Low Complexity MPC-DSVPWM for Current Control of PMSM Using Neural Network Approach," *IEEE Access*, vol. 10, pp. 132596–132607, 2022.

[19] H. A. G. Al-kaf, S. S. Hakami, L. M. Halabi and K. -B. Lee, "Model Predictive Current Control Using Single Layer Neural Network for PMSM Drives," *2022 IEEE Energy Conversion Congress and Exposition (ECCE)*, Detroit, MI, USA, 2022, pp. 1-5.

[20] Simon Haykin, Neural Networks and Learning Machines. Upper Saddle River, NJ: *Prentice Hall*, 2008